

Unsupervised learning of control signals and their encodings in *C. elegans* whole-brain recordings

Charles Fieseler^a, Manuel Zimmer^b, and J. Nathan Kutz^c

^a, ¹Department of Physics, University of Washington, Seattle, WA 98195; ^bResearch Institute of Molecular Pathology, Vienna, Austria; ^cDepartment of Applied Mathematics, University of Washington, Seattle, WA 98195

This manuscript was compiled on August 26, 2019

1 **Recent whole brain imaging experiments in *C. elegans* have revealed**
2 **that the neural connectomic dynamics live on a low dimensional man-**
3 **ifold with stereotyped transitions between behaviors. Typical theo-**
4 **retical efforts use data to produce a set of local linear models char-**
5 **acterizing the data, but it is unknown how a single, global neural**
6 **network model can generate the observed dynamics. We propose in-**
7 **stead a control framework to achieve a global model of the dynamics,**
8 **whereby underlying linear dynamics is actuated by sparse control**
9 **signals. The method learns the control signals in an unsupervised**
10 **way from data, then uses *Dynamic Mode Decomposition with control***
11 **(DMDc) to create the first global, linear dynamical system that can re-**
12 **construct whole-brain imaging data. These internally generated con-**
13 **trol signals are shown to be implicated in transitions between behav-**
14 **iors. In addition, we analyze the time-delay encoding of these control**
15 **signals, both reproducing known neural encodings and showing that**
16 **these transitions can be predicted from previously unknown neurons.**
17 **Moreover, our decomposition method allows one to understand the**
18 **observed nonlinear global dynamics instead as linear dynamics with**
19 **control. The proposed mathematical framework is generic and can**
20 **be generalized to other neurosensory systems, potentially revealing**
21 **transitions and their encodings in a completely unsupervised way.**

C. elegans | Control | DMD | ...

1 **T**he nematode *Caenorhabditis elegans* (*C. elegans*) is an
2 ideal model organism as it is comprised of only 302
3 sensory, motor and inter-neurons whose stereotyped electro-
4 physical connections (i.e. its connectome) are known from
5 serial section electron microscopy (1). Indeed, *C. elegans* is per-
6 haps the simplest biophysical organism to display many of the
7 hallmark features of high-dimensional networked biological sys-
8 tems, including the manifestation of low-dimensional patterns
9 of activity associated with functional behavioral responses.
10 Thus the nervous system encodes behavior by reducing the
11 high-dimensional representation of the environmental stimulus
12 into a much lower representations of motor command (2–6).
13 Low dimensional representations have been separately con-
14 sidered in posture (behavioral) analysis (7, 8) as well as in
15 the static analysis of calcium imaging data (9, 10). Under-
16 standing the computational processing that transforms sensory
17 input into motor representations requires the ability to record
18 the activity of sensory neurons, decision-making circuits, and
19 motor circuits in a behaving animal, something that is now
20 largely available with modern imaging of *C. elegans*. Real-
21 time, whole-brain imaging of these non-spiking neurons allows
22 for data-driven discovery of the governing dynamics of the
23 system and the low-dimensional manifold (coordinates) on
24 which neural activity exists (11). In this work, we exploit this
25 new, whole-brain imaging technology to posit a data-driven
26 model of neurosensory integration in *C. elegans*, showing that a
27 global, linear control framework alone explains and reproduces

much of the activity of the network.

28
29 It has long been observed that *C. elegans* produces a small
30 number of stable discrete behaviors (e.g. forward and back-
31 ward motion, and turns), and that these behaviors change
32 both spontaneously and very quickly in response to external
33 stimuli and/or stimulation of even a single neuron (12–14). A
34 potential dynamical systems explanation for this observation
35 is that of discrete behaviors as fixed points on an underlying
36 manifold with some transition signals that move the system
37 between them. A purely linear model cannot produce multiple
38 fixed points, but switching (hybrid) linear dynamical systems
39 methods (15–18) circumvent this by segmenting the dynamics
40 into patches with different dynamics (and thus different fixed
41 points) in each patch. An alternate method uses different
42 phase loops and the phase along them to predict behavior,
43 producing conserved dynamics in a special phase space (19).
44 Recent efforts have also attempted to explicitly model the non-
45 linear connectomic dynamics (6, 20–25), but this has currently
46 been limited to subsets of neurons and has moreover had diffi-
47 culty capturing multiple behaviors. This work instead focuses
48 on how a single, global, neuron-level model with simple and
49 interpretable additions can capture the nonlinear dynamics

Significance Statement

Biological organisms are very well adapted to the environments they live in, and can perform tasks that even our most advanced engineered cannot. For example, the soil-dwelling nematode *C. elegans* lives in a noisy environment made of vastly differing materials and viscosities. Sensory stimuli come from many different channels, and yet this “worm” is able to consistently integrate them and react appropriately, all with only 302 neurons. We use data-driven techniques to analyze real-time neuronal, whole-brain recordings in order to understand the separation of the system into a simple intrinsic linear dynamics and a more complex set of internally generated control signals. Our 3-step modeling framework can reproduce whole-brain imaging datasets from initial conditions and an interpretable control signal using Dynamic Mode Decomposition with Control (DMDc). Biologists can use each step of our framework to learn, possibly in new organisms: 1) where behavioral transitions occur; 2) about the complexity of different behaviors; and 3) which neurons produce the transition signals. Theorists can use this framework to: 1) build low-dimensional models characterizing connectomic dynamics; 2) identify distinct system states; and 3) build closed-loop feedback models.

The authors declare no conflict of interest.

¹To whom correspondence should be addressed. E-mail: konda@uw.edu

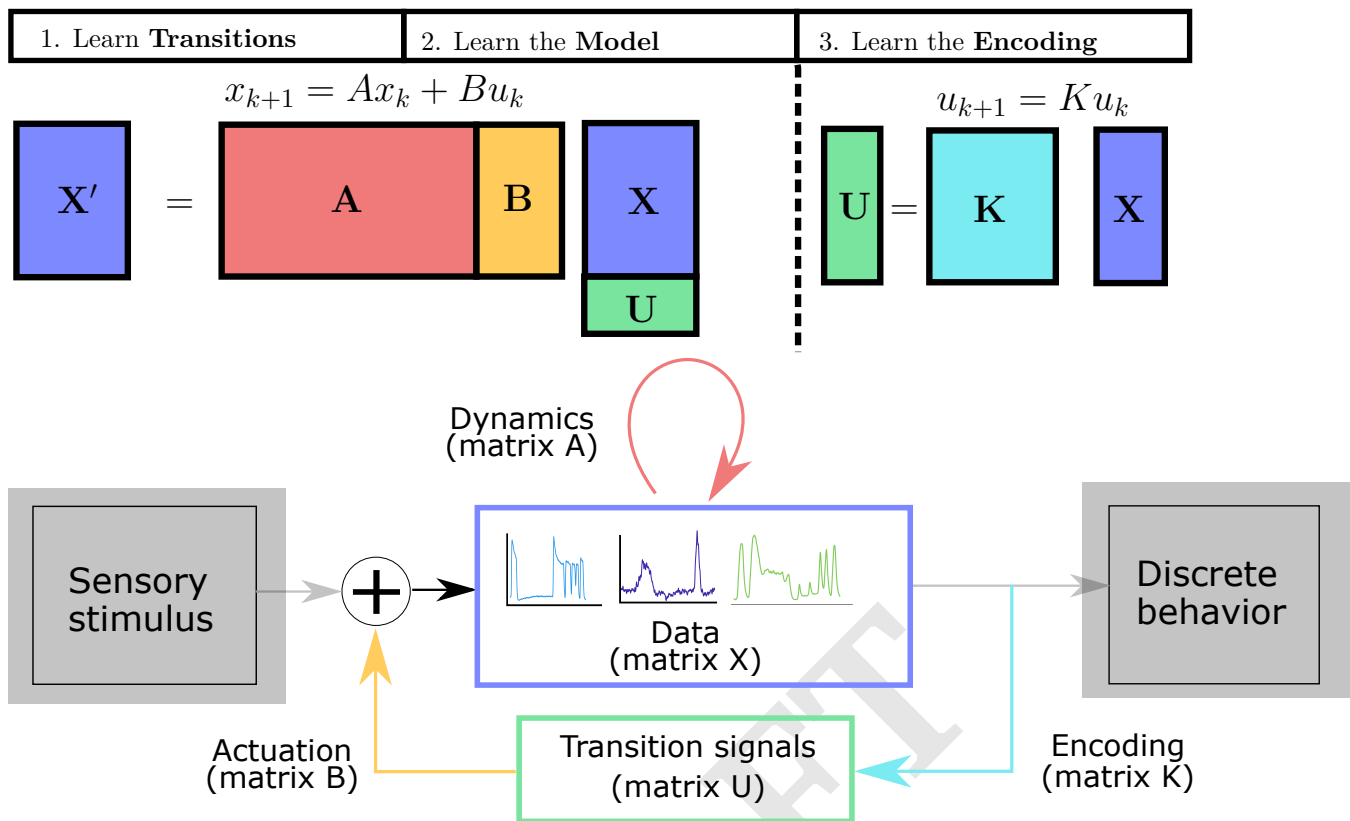


Fig. 1. A 3-step framework for modeling neurosensory integration. 1) Transition signals are learned from data with an assumption of linear dynamics. 2) A DMDc model is learned which uses dynamics, transition signals, and actuation. These are global models, and are capable of reconstructing much of the data dynamically from an initial state. 3) Where and at what timescales control signals are encoded in the neural activity is studied using sparse linear models.

50 simply by appropriate framing as a control problem.
 51 The recent availability of real-time calcium imaging data
 52 allows for a neuron-level data-driven approach. A full model of
 53 *C. elegans* neural activity should describe how multiple states
 54 are produced in a single network, and how dynamics operating
 55 at multiple scales are integrated to produce the states and
 56 transitions between them. This can be naturally expressed
 57 mathematically using control theory, with the data-driven
 58 method of *Dynamic Mode Decomposition with control* (DMDc)
 59 (4, 26) providing a regression framework for approximating
 60 linear control laws. We propose a mathematical framework
 61 for building such a model via a step-by-step analysis of the
 62 required components necessary for DMDc, generating inter-
 63 pretable and testable hypotheses at each step. This framework
 64 is able to 1) learn known and novel transition signals; 2)
 65 reconstruct entire datasets, including with multiple states,
 66 demonstrating that additional nonlinearities are not needed
 67 to describe many of the interactions in the system; and 3)
 68 analyze the timescales and locations of where these transition
 69 signals are encoded. We provide code written in MATLAB
 70 (27) for a full analysis pipeline that uses raw data and, if avail-
 71 able, external behavioral labels to discover both the intrinsic
 72 dynamics and the effects of control on the state of the system.

73 Data-Driven Methods

74 Our analysis relies on two established mathematical methods:
 75 DMDc and sparse optimization. A brief summary of each is
 76 given below.

Dynamic Mode Decomposition with control. Our data-driven
 strategy is based upon the *dynamic mode decomposition*
 (DMD). DMD provides a linear model for data matrices con-
 structed using temporal snapshots of the state space, $\mathbf{X} =$
 $[\mathbf{x}_1 \ \mathbf{x}_2 \ \dots \ \mathbf{x}_{m-1}]$ and $\mathbf{X}' = [\mathbf{x}_2 \ \mathbf{x}_3 \ \dots \ \mathbf{x}_m]$ where $\mathbf{x}_j = \mathbf{x}(t_j)$.
 Specifically, it finds the best fit linear dynamical system

$$\mathbf{X}' = \mathbf{A}\mathbf{X} \quad [1]$$

There are a number of variants for computing \mathbf{A} (4), with the
exact DMD simply positing $\mathbf{A} = \mathbf{X}'\mathbf{X}^\dagger$ where \dagger denotes the
 Moore-Penrose pseudo-inverse.

DMDc (26) capitalizes on all of the advantages of DMD
 and provides the additional innovation of being able to disam-
 biguate between the underlying dynamics and actuation. For a
 control input matrix $\mathbf{U} = [\mathbf{u}_1 \ \mathbf{u}_2 \ \dots \ \mathbf{u}_{m-1}]$ where $\mathbf{u}_j = \mathbf{u}(t_j)$,
 DMDc regresses instead to the linear control system

$$\mathbf{X}' = \mathbf{A}\mathbf{X} + \mathbf{B}\mathbf{U}. \quad [2]$$

Note that DMDc uses only snapshots in time of the state space
 and control input, making it compelling for systems whose
 governing equations are unknown. The DMDc equation is
 graphically represented in Fig. 1. The governing matrices (\mathbf{A}
 and \mathbf{B}) along with the control signal (\mathbf{U}) produce a predictive
 model, such that the state of the system far in the future
 can be predicted. For instance, the third time step can be
 estimated from the first via:

$$\mathbf{x}_3 = \mathbf{A}(\mathbf{A}\mathbf{x}_1 + \mathbf{B}\mathbf{u}_1) + \mathbf{B}\mathbf{u}_2 \quad [3]$$

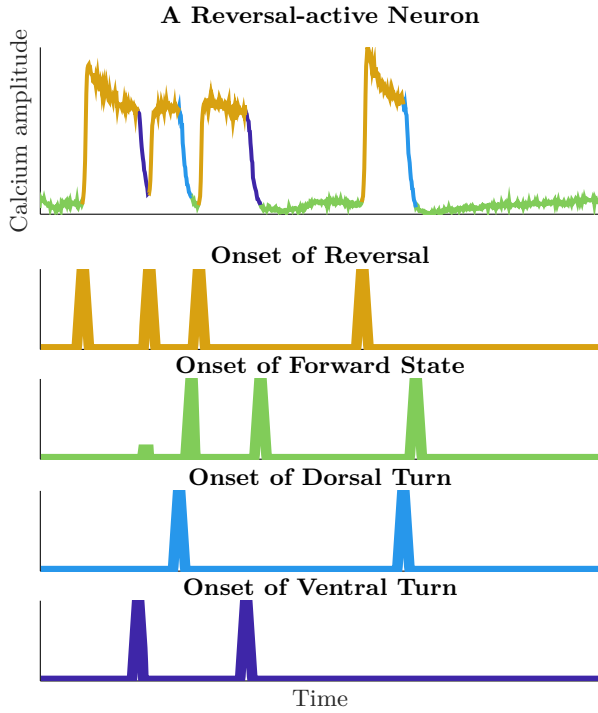


Fig. 2. Transition signals in *C. elegans*: Top: A calcium imaging trace of a neuron connected with the discrete reversal behavior. Behavioral labels are determined by experimentalists, as described in (9). Green=Forward; Yellow=Reversal; Dark Blue=Ventral Turn; Light Blue=Dorsal Turn. Below: These labels can be reframed as “onset” signals, and are characteristically sparse in time.

Algorithm 1 Unsupervised Learning of Control Signals

```

1: procedure LEARNCONTROLLERS( $r$ )
2:    $\mathbf{U}_0 := \text{InitializeU}(r)$ 
3:    $\mathbf{S} := \text{InitializeSparsityPattern}(\mathbf{U}_0)$ 
4:   for  $i \leftarrow 1, \text{MaxIter}$  do
5:      $\mathbf{A}, \mathbf{B} = \text{SolveAB}(\mathbf{X}, \mathbf{U}_{i-1})$  ▷ Solves eq. 2
6:      $\mathbf{U}_i = \text{SolveU}(\mathbf{X}, \mathbf{A}, \mathbf{B})$ 
7:      $\mathbf{S} = \text{UpdateSparsityPattern}(\mathbf{S}, \mathbf{U}_i)$ 
8:      $\mathbf{U}_i(\mathbf{S}) = 0$ 

```

(28). More recently, a convex relaxation of the ℓ_0 to an ℓ_1 norm is often solved (29), though this has been recently shown to make mistakes (30). We use a different approximation, the sequential least squares thresholding algorithm (31), which has been shown to converge to the minima of the original ℓ_0 problem (32). The code is outlined in algorithm 1 and more detail is given in the supplement. The matrix \mathbf{U} in this algorithm is additionally constrained to be positive, for better interpretability as “on” transition signals.

Variable selection via sparse linear models. If internally generated control signals are present, then there are two options: they are random and fundamentally unpredictable, or they are encoded in the network. Although there is almost certainly some amount of stochasticity in the true biological system, any encoding at all can be used to study the initiations and precursors of the behavior. Mathematically, this is a variable selection problem: given the data, which few neurons predict the transitions? In this paper we additionally use *time-delay embedding* where data from further in the past is utilized:

$$\mathbf{U} = \mathbf{K}_1 \mathbf{X}_1 + \mathbf{K}_2 \mathbf{X}_2 + \dots \quad [5]$$

There are multiple methods that are often used to perform this variable selection task (33). However, these methods may make mistakes in their selections (30), and in general it is unclear how unique the selection is. The behaviors of *C. elegans* have been well studied, and each onset is associated with well-known neurons. Variable selection methods will almost certainly discover these well-known neurons, but by exploring further in the “elimination path”, less obvious encodings can be discovered. Algorithmically, this is the sequential removal of the most important neuron for all time delays, and then a re-fitting of the sparse model. If the quality of the reconstruction does not degrade along the elimination path, the signal (\mathbf{U}) must be distributed throughout the data (\mathbf{X}). The quality of signal reconstruction is defined here as the number of false positives and false negatives in the reconstructed signal. Event detection is defined as a number of frames above a hard threshold, as shown in Fig. 5 and discussed in the supplement.

Results

Known transitions are discovered and characterized. Experimentalists have long separated behavior into discrete behaviors through careful study of individual neurons. However, open questions remain about the number of behaviors that exist and how discrete they are. Some works have posited up to six forward motion states and three reversal states, multiple turning subtypes, and even a continuum of behaviors (34). As Fig. 3 shows, using unsupervised optimization three behavioral onsets can be discovered: Reversal, and Dorsal and

Figure 4 refers to “full reconstructions” of the datasets, i.e. the prediction of snapshots up to 3000 time steps in the future given the initial data snapshot (\mathbf{x}_1) and the full time series of the control signals (\mathbf{U}).

Learning control signals via sparse optimization. The DMDc algorithm requires knowledge of the linear control signals \mathbf{U} . Expert-identified state labels and an example neuron that displays strong state-dependent behavior are shown in figure 2. However, these are only available because of the decades of *C. elegans* experimental work identifying 1) discrete behavioral states and 2) the command neurons for each activity. For new organisms, and in order to generate hypotheses about potential new states in *C. elegans*, the unsupervised problem, i.e. learning the signal directly from data, is of critical interest.

DMDc (2) can be thought of as an error minimization problem over the dynamics matrices, \mathbf{A} and \mathbf{B} . If the control signal is unknown, the minimization must be extended to the control signal \mathbf{U} itself. However, there is now a trivial solution where the control signal dominates the model: $\mathbf{X}_2 = \mathbf{B}\mathbf{U}$ with $\mathbf{A} = 0$. For this reason, an assumption must be made about the control signals. In this case, the statement that these signals are sparse is directly biologically interpretable, and means that the transitions between states should be rare as a percentage of frames. This “sparsity constraint” can be directly expressed in the language of optimization, i.e. the ℓ_0 norm:

$$\min_{\mathbf{A}, \mathbf{B}, \mathbf{U}} \left[\|\mathbf{A}\mathbf{X}_1 + \mathbf{B}\mathbf{U} - \mathbf{X}_2\|_2 + \lambda \|\mathbf{U}\|_0 \right] \quad [4]$$

Directly solving this optimization problem is extremely difficult, although there are efficient algorithms in certain cases

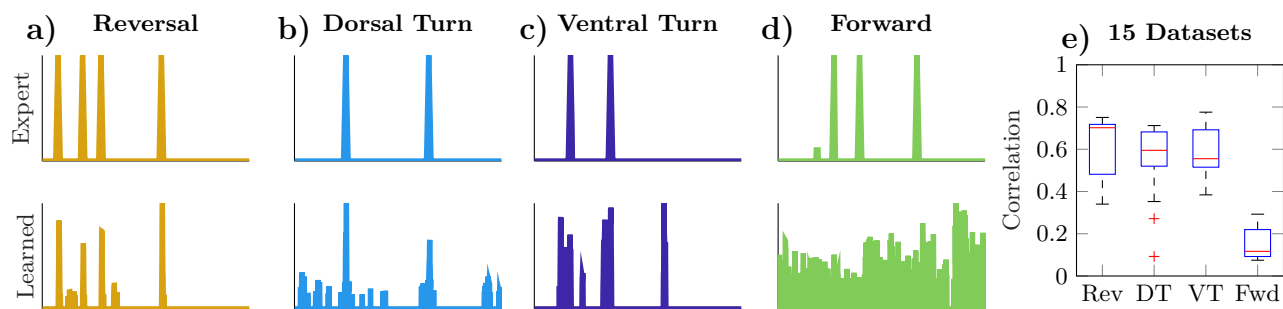


Fig. 3. Control signals can be learned from data via algorithm 1. a-d) The onset of well-known states as determined by experts (above) and as learned (below). e) Correlation between expert and learned signals across 15 individual datasets. Reversals (Rev), Dorsal (DT) and Ventral Turns (VT) are consistently learned, but Forward state (Fwd) onsets are never significant.

178 Ventral turns. In particular, the single Reversal onset signal
 179 for each individual suggests that this transition is fundamen-
 180 tally the same within individuals, with variability produced by
 181 activation amplitude not a different direction in neuron-space.

182 However, in no individuals could a signal correlated to the
 183 onset of Forward motion be discovered. This lack of a discov-
 184 ery can be interpreted as the underlying neural mechanism
 185 producing forward motion being fundamentally different. It is
 186 well known that different, dedicated sub-networks of neurons
 187 are active in forward and backwards motion (1), but they are
 188 often modeled as mirror images of each other (25). This result
 189 implies that for the onset of these behaviors, forward motion
 190 is significantly more complex than reversals, not simply that
 191 the underlying networks are physically distinct.

192 **A global, linear system with control reconstructs entire time**
 193 **series.** The manifold observed in *C. elegans* neural dynamics
 194 cannot be described by a purely linear model due to the pres-
 195 ence of multiple stable global behaviors, as shown in Fig.
 196 4.b. Specifically, linear models can only admit a single fixed
 197 state. However, the majority of neurons can be reconstructed
 198 using our *controlled, global, linear* dynamical system due to
 199 the sparse transition signals as shown in Fig. 4.c for expert
 200 hand-labeled signals and Fig. 4.d for signals learned from data.
 201 Each time snapshot of this data is reconstructed analogously
 202 to equation 3, and then projected onto the two dominant PCA
 203 modes of the original data so that each panel in Fig. 4.a-d is
 204 in the same coordinate space. Because this is a global linear
 205 model that uses a single framework for the entire state space,
 206 the need for additional nonlinear modeling can be constrained
 207 to particular groups of neurons and well-defined time windows.

208 In particular, across individuals the reversal class of neu-
 209 rons is captured very well by the supervised control signal
 210 as shown in Fig. 4.j and thus, up to encoding the transition
 211 signal itself, the relevant subnetwork does not appear to re-
 212 quire nonlinearities. This means that future efforts related to
 213 nonlinear modeling should concentrate on the small window
 214 of time during the onset of the behavior, instead of the entire
 215 neural trace where linear models hold. In addition, the type of
 216 nonlinearity required to more fully model this class of neurons
 217 is characterized: fast and short-lived spike-like activations.

218 Turns are also largely captured, as shown by the high cor-
 219 relation for the light and dark blue boxplots. The neurons
 220 involved in turning have a large number of smaller events, as
 221 shown in the SMDDL reconstruction Fig. 4.f; these do not
 222 lead to one of the four state transitions identified by experi-

223 mentalists in this dataset (CITE timescale nesting paper?),
 224 but may correspond to an additional state as discussed in the
 225 supplement. However, the unsupervised method does pick up
 226 on these smaller events and reconstructs them well Fig. 4.h,
 227 but over all datasets there is much more variability as shown
 228 in Fig. 4.j.

229 The last group of neurons, those related to forward motion,
 230 has a very large variability of correlation between the data
 231 and reconstructions, implying that this state requires nontriv-
 232 ial nonlinearities throughout the time series to capture. It
 233 may be continuously parametrized instead of a simple “on”
 234 transition signal at the onset, for example by speed, steering
 235 (35), or tracking (36). Some recent experimental work (37)
 236 characterizes this asymmetry between Forward and Reversal
 237 states as due to intrinsic bias towards the Forward state, and
 238 this result is consistent with that interpretation but adds that
 239 the Forward state is significantly more complex.

240 To further characterize the effects of the control signals on
 241 the ability of this framework to capture the neural dynamics,
 242 partial models were created with a subset of control signals.
 243 Expert-labeled partial models are shown in Fig. 4.k. Adding
 244 Reversal-onset signals alone does not produce a model that
 245 captures the data better than a straight-line fit to the data, but
 246 the combination of Reversal and Turning signals is significantly
 247 better. The subsequent additional of Forward control signals
 248 is, remarkably, useless and is another line of evidence showing
 249 that this behavior is truly different from the simpler Reversal
 250 state.

251 **Transitions are encoded in previously unknown neurons.**

252 Having shown the control signals to contribute significantly
 253 to the reconstruction of the data, we reconstruct the control
 254 signals themselves using time-delay data matrices and sparse
 255 linear models as shown in step 3 of Fig. 1 according to equa-
 256 tion 5. As described in (10), each of the four interpretable
 257 transition signals shown in figure 3 are hand-labeled using
 258 the activity of certain well-known neurons. Thus, it is not
 259 surprising that these signals can be reconstructed from data
 260 when those well-known neurons are included. In particular, as
 261 they were used to define the Dorsal Turn behavioral states, an
 262 excellent validation is that the SMDDL/R pair of left/right
 263 neurons consistently encodes this control signal, as Fig. 5.a
 264 shows.

265 However, as the elimination path is explored further, it
 266 is revealed that these well-known neurons can be eliminated
 267 from the sparse models and the transition signals can still be

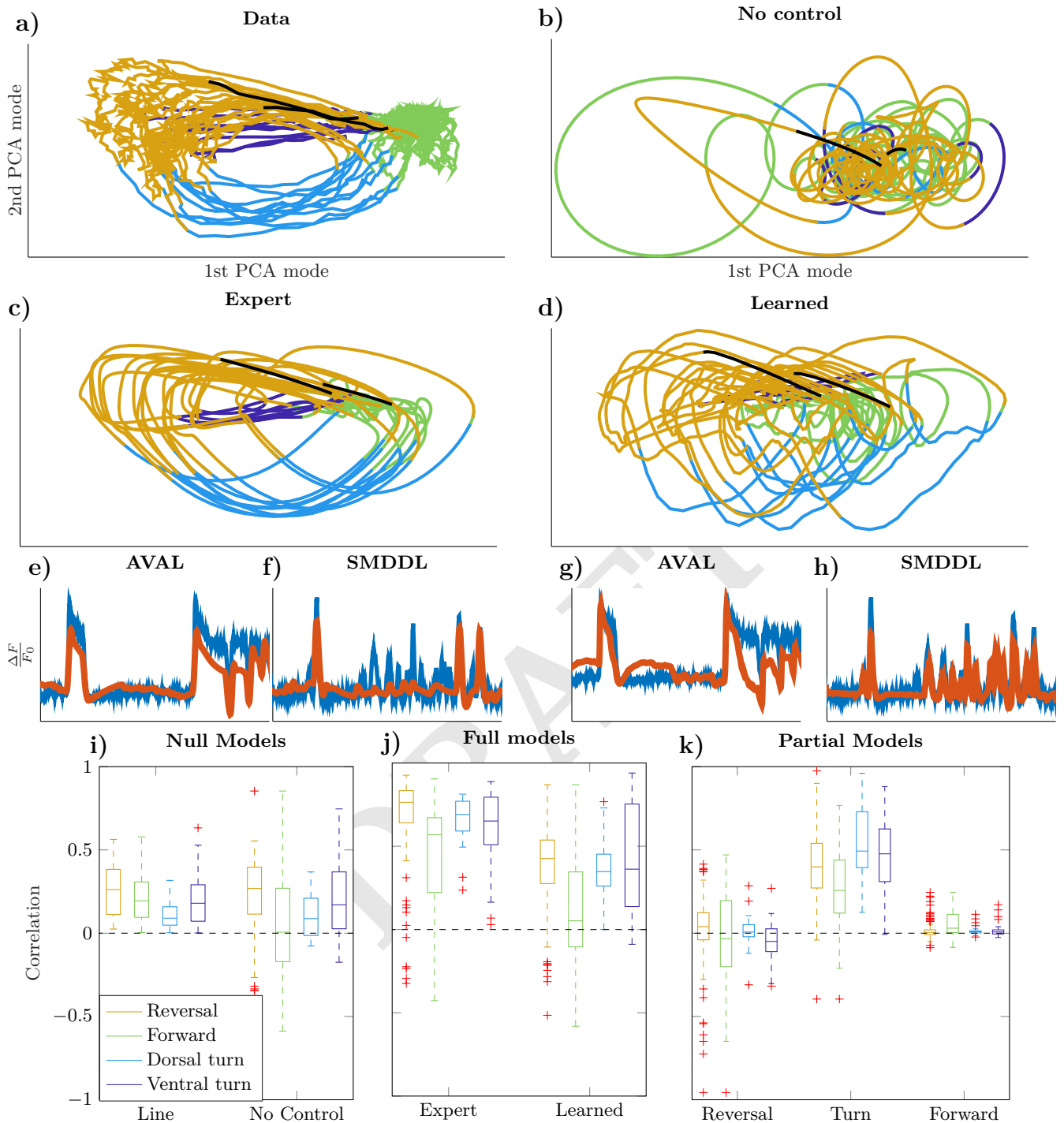


Fig. 4. 2d PCA projections of a) data, b) an uncontrolled “null” model, c) a “supervised” model using expert-determined control signals, and d) an “unsupervised” model that uses control signals learned via algorithm 1. The governing equations matrices in are all learned from data, either uncontrolled (b, Equation 1) or controlled (c-d, Equation 2). These data are color-coded by state: Black for Unknown, Yellow for Reversal neurons, Green for Forward, and Light (Dark) Blue for Dorsal (Ventral) turns. e-f) Example neuron datasets with reconstructions from the supervised model. A reversal-active (AVAL) and a Dorsal-Turn-active neuron (SMDDL) are shown. g-h) The same neurons shown with reconstructions from the unsupervised model. i-k) Correlations across datasets between data and reconstructions, split up into 4 different neuron groupings for interpretability. i) Baseline null models. The left-hand side is simply fitting a straight line to a neural trace. The right-hand side corresponds to the uncontrolled model in panel (b), and is generally worse than a straight-line fit. j) Full models with either expert/supervised control signals, (c) above, or learned/unsupervised control signals, (d) above. For each neuron grouping the expert signals produce significantly better fits. k) Partial supervised models, as more signals are added. Shown are additive improvements, i.e. how much better each partial model is than the one immediately to the left. Specifically, “baseline” of a straight-line fit is subtracted from the Reversal (left-hand side) set, and the Reversal + Turn model correlations are subtracted from the cumulative Forward (right-hand side) set, which has Reversal + Turn + Forward control signals.

268 reconstructed as shown in 5.b. Indeed, Fig. 5.a and and 5.b
 269 look nearly identical, and Fig. 5.c quantifies this using the

percentage of false positives and negatives. Fig. 5.c also shows
 more of the elimination path and when the reconstructions

270
 271

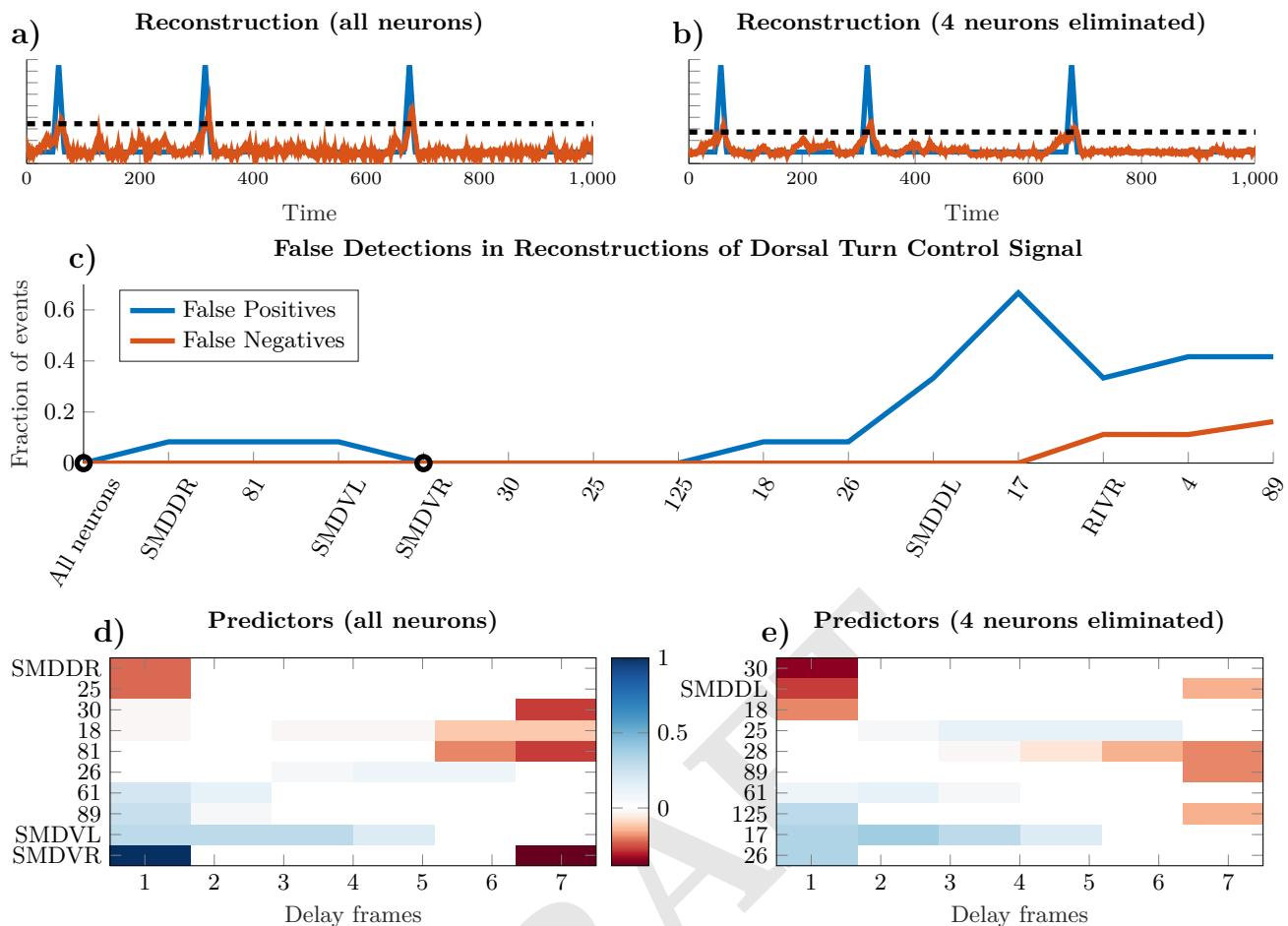


Fig. 5. a-b) Signal reconstructions via linear encoding on the data including time delays, with all neurons (a) or 4 neurons removed (b). Event detection is determined via a simple hard threshold for each signal, as shown by the dotted line. c) Neurons are eliminated in order of the largest magnitude given to them by the linear model. The number of false detections increases significantly only after 8 neurons have been removed. d-e) The weights given to the top 10 most important neurons for different iterations. Even though the prediction is very good as measured by the false positive and negative rates, many of the neurons determined to be important are different.

272 finally break down. Fig. 5.d and 5.e show the how \mathbf{K} matrices
 273 in equation 5 change as neurons are removed. Taken together,
 274 these results reveal previously unknown neurons that can
 275 successfully predict control signals shown to be important
 276 to reconstructing the full neural manifold. However, only
 277 rows with names are neurons that have been connected to the
 278 stereotyped *C. elegans* connectome and can thus be identified
 279 across individuals; rows with numbers cannot be so compared.
 280 This work identifies sets of unknown neurons that could be
 281 investigated in further experiments, and the timescale at which
 282 they are relevant.

283 Discussion

284 We have presented the first data-driven model that uses a single
 285 set of intrinsic dynamics that can reconstruct the multiple
 286 behavioral regimes present in a real animal and transitions
 287 between them. The fact that this controlled linear model
 288 accurately reproduces both short and long time-scale dynamics
 289 places clear restrictions on the need, specifically the lack
 290 thereof, for nonlinearities in this system, and provides hypotheses
 291 about the neurons that may contain those nonlinearities
 292 and their role in the global dynamics of the system. In addition,
 293 we have embedded this model in a mathematical framework

of feedback and control, which can be generalized to other
 organisms or to include hypothesized nonlinearities.

Much excitement has been generated by the availability
 of the *C. elegans* physiological connectome, and one hope of
 data-driven modeling efforts is to produce a functional connectome
 that can complement the physiological data. The DMDc in this paper
 is similar to several algorithms in the engineering literature that
 attempt similar network reconstruction tasks, namely System
 Identification (38). One strategy to fully disambiguate the effects
 of the intrinsic dynamics and the external control signals uses
 known external perturbations should be applied and the system
 response measured. Such perturbations are not generally available
 in biological systems and thus the data collected are “uninformative”
 (39) in the sense that the underlying structure cannot be determined.

A limitation of this model is that it is not generative; it
 cannot be used to predict a system response that includes
 transitions to novel stimuli. To accomplish this, the transition
 signals must be written as a function of the data. Step three of
 our method does this with a linear encoding and demonstrates
 that the signals can be successfully reconstructed with all
 neurons to a certain level of accuracy. If this level of accuracy
 were sufficient, then the system would be fully linear and an

317 uncontrolled model would produce a good reconstruction, as
318 is clearly not the case. Recent methods for incorporating
319 nonlinearities into controlled systems (e.g. (31, 40)) have the
320 potential to create a fully closed-loop feedback system and
321 this is an active area of further research.

322 A potential criticism of this method is that we have used
323 discrete labeled states in our model, despite ongoing debate re-
324 garding how uniform “states” in *C. elegans* are across instances,
325 and if they should be subdivided or are simply continuous
326 (34). We have contributed to this debate by providing evi-
327 dence that the reversal and turn states in fact appear to be
328 simple and have well-defined initiation signals, but that the
329 forward “state” is much more complex. We argue that this is
330 an example of a strength of this methodology: the fact that
331 a state cannot be reconstructed gives additional information
332 about that state, and about its complexity in relation to other
333 states.

334 An alternate approach to modeling complex systems in
335 order to understand structure is to use locally linear models
336 (15–18). In this methodology, the initial network as described
337 by the matrix \mathbf{A}_i is replaced by a new matrix, \mathbf{A}_{i+1} , at
338 certain change points. These have achieved great success in
339 reconstructing nonlinear datasets and is an active field in
340 machine learning research. However, it is difficult to interpret
341 what such a replacement of the underlying dynamics would
342 mean biologically, particularly if many separate matrices \mathbf{A}_i
343 are required. On the other hand, the language of control
344 theory from engineering meshes directly with the biological
345 intuition that certain states are initiated by relatively unique
346 signals produced by a small number of neurons. We believe
347 that our framework for constructing a single, global model of
348 the dynamics of this neural system is promising not only in
349 its ready generalizability to include nonlinearities, but also in
350 its biological interpretability.

351 We have produced the first, to our knowledge, global data-
352 driven model of both the intrinsic and control dynamics of *C.*
353 *elegans*. We hope this work can contribute to the realization
354 of fully in-silico ablation and actuation experiments, the holy
355 grail of *C. elegans* simulation.

356 References.

357 1. White JG, Southgate E, Thomson JN, Brenner S (1986) The structure of the nervous
358 system of the nematode *Caenorhabditis elegans*. *Philos Trans R Soc Lond B Biol Sci*
359 314(1165):1–340.
360 2. Roberts WM, et al. (2016) A stochastic neuronal model predicts random search behaviors at
361 multiple spatial scales in *C. elegans*. *Elife* 5.
362 3. Liu H, Kim J, Shlizerman E (2017) Functional connectomics from data: Probabilistic graphical
363 models for neuronal network of *C. elegans*. *arXiv preprint arXiv:1711.00193*.
364 4. Kutz JN, Brunton SL, Brunton BW, Proctor JL (2016) *Dynamic mode decomposition: data-*
365 *driven modeling of complex systems*. (SIAM) Vol. 149.
366 5. Kunert-Graf JM, Shlizerman E, Walker A, Kutz JN (2017) Multistability and long-timescale
367 transients encoded by network structure in a model of *C. elegans* connectome dynamics.
368 *Frontiers in computational neuroscience* 11:53.
369 6. Fieseler C, Kunert-Graf J, Kutz JN (2018) The control structure of the nematode *Caenorhabditis*
370 *elegans*: Neuro-sensory integration and proprioceptive feedback. *Journal of Biomechanics*
371 74:1–8.
372 7. Stephens GJ, Johnson-Kerner B, Bialek W, Ryu WS (2008) Dimensionality and dynamics in
373 the behavior of *C. elegans*. *PLoS computational biology* 4(4):e1000028.
374 8. Stephens GJ, de Mesquita MB, Ryu WS, Bialek W (2011) Emergence of long timescales and
375 stereotyped behaviors in *Caenorhabditis elegans*. *Proceedings of the National Academy of*
376 *Sciences* 108(18):7286–7289.
377 9. Kato S, et al. (2015) Global brain dynamics embed the motor command sequence of
378 *Caenorhabditis elegans*. *Cell* 163(3):656–669.
379 10. Nichols AL, Eichler T, Latham R, Zimmer M (2017) A global brain state underlies *C. elegans*
380 sleep behavior. *Science* 356(6344):eaam6851.
381 11. Venkatachalam V, et al. (2016) Pan-neuronal imaging in roaming *Caenorhabditis elegans*.
382 *Proceedings of the National Academy of Sciences* 113(8):E1082–E1088.
383 12. Kocabas A, Shen CH, Guo ZV, Ramanathan S (2012) Controlling interneuron activity in
384 *Caenorhabditis elegans* to evoke chemotactic behaviour. *Nature* 490(7419):273.

385 13. Leifer AM, Fang-Yen C, Gershow M, Alkema MJ, Samuel AD (2011) Optogenetic manipulation
386 of neural activity in freely moving *Caenorhabditis elegans*. *Nature methods* 8(2):147.
387 14. Nagel G, et al. (2005) Light activation of channelrhodopsin-2 in excitable cells of *Caenorhabditis*
388 *elegans* triggers rapid behavioral responses. *Current Biology* 15(24):2279–2284.
389 15. Linderman S, Adams R (2014) Discovering latent network structure in point process data in
390 *International Conference on Machine Learning*, pp. 1413–1421.
391 16. Linderman SW, et al. (2016) Recurrent switching linear dynamical systems. *arXiv preprint*
392 *arXiv:1610.08466*.
393 17. Costa AC, Ahamed T, Stephens GJ (2019) Adaptive, locally linear models of complex dynam-
394 ics. *Proceedings of the National Academy of Sciences* 116(5):1501–1510.
395 18. Linderman SW, Nichols AL, Blei DM, Zimmer M, Paninski L (2019) Hierarchical recurrent
396 state space models reveal discrete and continuous dynamics of neural activity in *C. elegans*.
397 *bioRxiv* p. 621540.
398 19. Brennan C, Proekt A (2019) A quantitative model of conserved macroscopic dynamics pre-
399 dicts future motor commands. *eLife* 8:e46814.
400 20. Kunert J, Shlizerman E, Kutz JN (2014) Low-dimensional functionality of complex network
401 dynamics: Neurosensory integration in the *Caenorhabditis elegans* connectome. *Physical*
402 *Review E* 89(5):052805.
403 21. Mujika A, Leškovský P, Álvarez R, Otaduy MA, Epelde G (2017) Modeling behavioral experi-
404 ment interaction and environmental stimuli for a synthetic *C. elegans*. *Frontiers in neuroinfor-*
405 *matics* 11:71.
406 22. Costalago-Meruelo A, et al. (2018) Emulation of chemical stimulus triggered head movement
407 in the *C. elegans* nematode. *Neurocomputing* 290:60–73.
408 23. Izquierdo EJ (2018) Role of simulation models in understanding the generation of behavior in
409 *C. elegans*. *Current Opinion in Systems Biology*.
410 24. Gleeson P, Lung D, Grosu R, Hasani R, Larson SD (2018) c302: a multiscale framework for
411 modelling the nervous system of *Caenorhabditis elegans*. *Philosophical Transactions of the*
412 *Royal Society B: Biological Sciences* 373(1758):20170379.
413 25. Boyle JH, Berri S, Cohen N (2012) Gait modulation in *C. elegans*: an integrated neurome-
414 chanical model. *Frontiers in computational neuroscience* 6:10.
415 26. Proctor JL, Brunton SL, Kutz JN (2016) Dynamic mode decomposition with control. *SIAM*
416 *Journal on Applied Dynamical Systems* 15(1):142–161.
417 27. Fieseler C (2019) Celegansmodel.
418 28. Jewell S, Witten D (2018) Exact spike train inference via 0 optimization. *The annals of applied*
419 *statistics* 12(4):2457.
420 29. Donoho DL (2006) For most large underdetermined systems of linear equations the minimal
421 1-norm solution is also the sparsest solution. *Communications on Pure and Applied Mathe-*
422 *matics: A Journal Issued by the Courant Institute of Mathematical Sciences* 59(6):797–829.
423 30. Su W, Bogdan M, Candès E, et al. (2017) False discoveries occur early on the lasso path.
424 *The Annals of Statistics* 45(5):2133–2150.
425 31. Brunton SL, Proctor JL, Kutz JN (2016) Sparse identification of nonlinear dynamics with con-
426 trol (sindy). *IFAC-PapersOnLine* 49(18):710–715.
427 32. Zhang L, Schaeffer H (2018) On the convergence of the sindy algorithm. *arXiv preprint*
428 *arXiv:1805.06445*.
429 33. Tibshirani R (1996) Regression shrinkage and selection via the lasso. *Journal of the Royal*
430 *Statistical Society: Series B (Methodological)* 58(1):267–288.
431 34. Szigeti B, Deogade A, Webb B (2015) Searching for motifs in the behaviour of larval
432 *Drosophila melanogaster* and *Caenorhabditis elegans* reveals continuity between behavioural
433 states. *Journal of the Royal Society Interface* 12(113):20150899.
434 35. Iino Y, Yoshida K (2009) Parallel use of two behavioral mechanisms for chemotaxis in
435 *Caenorhabditis elegans*. *Journal of Neuroscience* 29(17):5370–5380.
436 36. Luo L, Clark DA, Biron D, Mahadevan L, Samuel AD (2006) Sensorimotor control during
437 isothermal tracking in *Caenorhabditis elegans*. *Journal of experimental biology*
438 209(23):4652–4662.
439 37. Kawano T, et al. (2011) An imbalancing act: gap junctions reduce the backward motor circuit
440 activity to bias *C. elegans* for forward locomotion. *Neuron* 72(4):572–586.
441 38. Ljung L (2001) System identification. *Wiley Encyclopedia of Electrical and Electronics Engi-*
442 *neering*.
443 39. Angulo MT, Moreno JA, Lippner G, Barabási AL, Liu YY (2017) Fundamental limitations
444 of network reconstruction from temporal data. *Journal of the Royal Society Interface*
445 14(127):20160966.
446 40. Williams MO, Kevrekidis IG, Rowley CW (2015) A data-driven approximation of the koop-
447 man operator: Extending dynamic mode decomposition. *Journal of Nonlinear Science*
448 25(6):1307–1346.

ACKNOWLEDGMENTS. Please include your acknowledgments
449 here, set in a single paragraph. Please do not include any acknowl-
450 edgments in the Supporting Information, or anywhere else in the
451 manuscript.
452